

CONTACT DISORDER AND FORCE DISTRIBUTION IN GRANULAR MATERIALS.

DESORDRE DE CONTACT ET DISTRIBUTION DES FORCES DANS LES MATERIAUX GRANULAIRES.

Jean-Noël ROUX

Laboratoire Central des Ponts et Chaussées,
58 boulevard Lefèbvre, 75732 Paris cedex 15, France

ABSTRACT: Thanks to extensive numerical simulations of a simple two-dimensional model of a granular packing, we identify a characteristic length for stress homogeneity that is significantly larger than the grain size, and accurately compute the contact force distribution. The effects of load orientation (biaxial test) are studied, and the influence of some basic simplifying assumptions (small displacements, no friction...) is discussed, which allows us to shed some light on the possible microscopic origins of some generic mechanical behaviours of granular materials.

RESUME: Une étude systématique, par simulations numériques, d'un modèle simple d'assemblage granulaire bidimensionnel, nous conduit à l'identification d'une longueur caractéristique de l'homogénéité des contraintes nettement plus grande que la taille du grain, et à un calcul précis de la distribution des forces de contact. L'évaluation de l'influence de l'orientation (test biaxial) du chargement, et la discussion des conséquences de quelques hypothèses simplificatrices (petits déplacements, absence de frottement...) fournissent un éclairage des possibles origines microscopiques de certains comportements mécaniques génériques des granulats.

1 INTRODUCTION.

One specific feature of dense granular media, as distinguished from other disordered mechanical systems, is the unilaterality and extremely short range of the particle interaction. Two neighbouring grains, if they touch, may strongly repel each other, but once the contact opens, which requires but an arbitrarily small motion, no force is transmitted any longer. In a seemingly homogeneous well compacted medium, opening and closing of contacts leads to a characteristic heterogeneity (1-4) of stress transport: forces appear to be localized on preferred paths (or 'force chains'), while some grains carry no load ('arching effect'). Defining a Represent-

tative Volume Element (RVE), a crucial step (5) in the derivation of macroscopic constitutive laws, is not straightforward.

The model we study here was designed (8) to study the consequences of this basic grain-level phenomenon, that might be called *contact disorder*, in a situation as simple as one might conceive of. It lends itself to a novel and powerful numerical method, that enables us to repeat the calculations for many different (random) initial geometries, various boundary conditions and large enough system sizes. This, after its introduction in section 2, and a presentation of its mechanical properties (sections 3 and 4), and of the numerical method (section 5), allows us (as explained in part 6) to study the large system

limit with good accuracy. Section 7 presents the results of a biaxial test (macroscopic constitutive law, distribution of contact forces), and the conclusive section (part 8) discusses the general relevance of the model and the role of its basic assumptions.

2 THE MODEL

Consider a close-packed 2D assembly of n discs of diameter a , on a regular triangular lattice. To any disc i , assign a number δ_i , that is randomly picked up with uniform probability in the interval $[0, \alpha]$, with $0 \leq \alpha \ll 1$, and reduce its diameter to $a_i = a(1 - \delta_i)$. This (fig. 1) is the reference configuration of the system, from which displacements are evaluated. Then, submitting it to

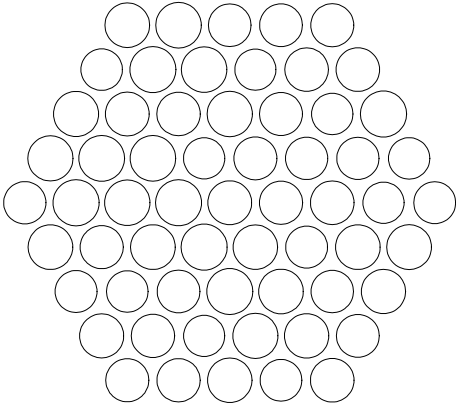


Figure 1: A hexagonal sample. Intergranular gaps are widened on the figure.

some given load, search for equilibrium displacements and contact forces, under the following three assumptions.

1. discs are rigid
2. friction is ignored
3. one may use the approximation of small displacements (ASD).

Assumption 2 means that the force \mathbf{F}_{ij} exerted by any disc i onto its neighbour j is carried by the unit vector \mathbf{n}_{ij} pointing from the centre of i to the centre of j : one has $\mathbf{F}_{ij} = f_{ij}\mathbf{n}_{ij}$, with $f_{ij} > 0$. According to assumption 1, the contact law relating f_{ij} to the interstitial thickness h_{ij} (initially equal

to $h_{ij}^0 = (\delta_i + \delta_j)a/2$) is the Signorini condition:

$$\begin{cases} f_{ij} = 0 & \text{if } h_{ij} > 0 \\ f_{ij} \geq 0 & \text{if } h_{ij} = 0 \end{cases} \quad (1)$$

The ASD (assumption 3) amounts to evaluate displacements and deformations to first order in α (regarded as infinitesimal), while positions and forces are evaluated on the reference configuration. In particular, any vector \mathbf{n}_{ij} stays parallel to one of the three vectors $\mathbf{n}_1(1, 0)$, $\mathbf{n}_2(\frac{1}{2}, \frac{\sqrt{3}}{2})$ and $\mathbf{n}_3(-\frac{1}{2}, \frac{\sqrt{3}}{2})$. h_{ij} is linearly related to the displacements:

$$\begin{aligned} h_{ij} &= h_{ij}^0 - \delta u_{ij}, \\ \text{with } \delta u_{ij} &= \mathbf{n}_{ij} \cdot (\mathbf{u}_i - \mathbf{u}_j). \end{aligned} \quad (2)$$

In the following, any such pair i, j of neighbours on the lattice is called a contact. N denoting the number of contacts, those are labelled by index l , $1 \leq l \leq N$, and one may write h_l , δu_l , \mathbf{n}_l , etc... Contact l is *closed* if $h_l = 0$. It is *active* if $f_l > 0$.

3 STRESSES AND STRAINS

In order to impose a state of uniform stress, several boundary conditions (BC) are used. One may specify the motion of the walls of a container, or exert some external forces on the grains near the boundary. If the sample shape paves the plane, periodic boundary conditions might also be implemented. For whatever BC, an overall, generalized displacement (or, respectively, force) is directly defined, and the conjugate generalized force (resp., displacement) identified on writing the work of external efforts. Those global static and kinematic parameters may respectively be interpreted as stress, σ , and strain, ϵ , tensors. We implement the $\overline{\text{BC}}$'s in such a way that the classical relationship (15)

$$\sigma = \frac{a}{A} \sum_{l=1}^N f_l \mathbf{n}_l \otimes \mathbf{n}_l \quad (3)$$

holds exactly, $A = \frac{Na^2}{2\sqrt{3}}$ being the sample surface area. (Compressions are counted positively). It is convenient to part contacts in three subsets C_k , $1 \leq k \leq 3$ (with $N/3$ of them, for large systems, in each) according

to which vector \mathbf{n}_k \mathbf{n}_l is parallel to. F_k denoting then the average of the contact forces in the set C_k , eqn. 3 becomes :

$$\begin{cases} \sigma_{11} = \frac{1}{a\sqrt{3}} \left(2F_1 + \frac{1}{2}(F_2 + F_3) \right) \\ \sigma_{12} = \frac{1}{2a} (F_2 - F_3) \\ \sigma_{22} = \frac{1}{2a} (F_2 + F_3) \end{cases} \quad (4)$$

which, conversely, may be written as

$$\begin{cases} F_1 = \frac{a\sqrt{3}}{2} \left(\sigma_{11} - \frac{1}{3}\sigma_{22} \right) \\ F_2 = a \left(\frac{\sigma_{22}}{\sqrt{3}} + \sigma_{12} \right) \\ F_3 = a \left(\frac{\sigma_{22}}{\sqrt{3}} - \sigma_{12} \right) \end{cases} \quad (5)$$

Such a linear relation giving the angular distribution of normal forces once $\underline{\sigma}$ is known was conjectured in the general case (15). It is automatically satisfied here because there are only three contact directions.

$(\delta u_l)_{1 \leq l \leq N}$ is an admissible set of normal relative displacements if it is compatible with some actual disc displacements and the BC. It is then associated with a value of ϵ . Similarly, $(f_l)_{1 \leq l \leq N}$ is an admissible set of contact forces if discs are in equilibrium, with some value of σ . For any such pair of relative displacements (superscript (1)) and contact forces (superscript (2)), one has the following form of Hill's lemma (5):

$$\sum_{l=1}^N f_l^{(2)} \delta u_l^{(1)} = A \underline{\sigma}^{(2)} : \underline{\epsilon}^{(1)}. \quad (6)$$

Now, due to lattice regularity, the replacement of any $f_l^{(2)}$ by the average $F_k^{(2)}$ whenever $l \in C_k$ yields another admissible set of contact forces, with the same $\underline{\sigma}^{(2)}$ (this property, in fact, guides the choice of a convenient implementation of the BC's). Defining then λ_k , for $1 \leq k \leq 3$, as the average of $\frac{\delta u_l}{a}$ over all $l \in C_k$, eqn. 6 entails

$$\underline{A \sigma}^{(2)} : \underline{\epsilon}^{(1)} = \frac{Na}{3} \sum_{k=1}^3 F_k^{(2)} \lambda_k^{(1)},$$

which, using eqn. 5, leads to the following kinematic analogue of eqn. 4:

$$\begin{cases} \epsilon_{11} = \lambda_1 \\ \epsilon_{12} = \frac{1}{\sqrt{3}} (\lambda_2 - \lambda_3) \\ \epsilon_{22} = \frac{1}{3} (-\lambda_1 + 2\lambda_2 + 2\lambda_3) \end{cases} \quad (7)$$

(Shrinking deformations are positive.)

4 EQUILIBRIUM STATE

The following properties stem from classical results in linear programming (a particular case of the Kuhn-Tucker theorem in convex optimization). Let us submit the system to a given external load. If m is the number of degrees of freedom, m -dimensional (generalized) displacement and external force vectors \vec{U} and \vec{F} may be defined. The value of \vec{F} is imposed. The impenetrability constraint may be written (see eqn. 2) as (summation over repeated indices implied in the sequel)

$$\mathcal{G}_{lj} \mathcal{U}_j \leq h_l^0, \quad (8)$$

involving an $N \times m$ matrix \mathcal{G} the transpose of which appears in the equilibrium requirement

$$\mathcal{G}_{lj} f_l = \mathcal{F}_j. \quad (9)$$

Let us consider problems \mathcal{P}_1 (unknown \vec{U}) and \mathcal{P}_2 (unknowns f_l)

$$\mathcal{P}_1 \begin{cases} \text{Maximize } \mathcal{F}_j \mathcal{U}_j \\ \text{with constraints: (8)} \end{cases}$$

$$\mathcal{P}_2 \begin{cases} \text{Minimize } f_l h_l^0 \\ \text{with constraints (9) and } f_l \geq 0 \end{cases}$$

\mathcal{P}_1 and \mathcal{P}_2 are *dual linear optimization problems*. To any solution \vec{U}^* to \mathcal{P}_1 corresponds a solution f^* to \mathcal{P}_2 , and reciprocally, such that

$$f_l^* (h_l^0 - \mathcal{G}_{lj} \mathcal{U}_j^*) = 0. \quad (10)$$

Conversely, displacements and contact forces satisfying the constraints of \mathcal{P}_1 and \mathcal{P}_2 and relation 10 are solutions to \mathcal{P}_1 and \mathcal{P}_2 . But, once constraints are satisfied, eqn. 10 is exactly equivalent to the Signorini condition, eqn. 1. Thus, *searching for an equilibrium state amounts to looking for solutions to \mathcal{P}_1 and \mathcal{P}_2* . Whenever \mathcal{P}_1 or \mathcal{P}_2 possess a solution, there exists a 'basic' solution, *i.e.*, located in a corner of the simplex of admissible variables, where a maximum set a inequality constraints are satisfied as equalities. The set C^* of active contacts corresponding to a basic solution to \mathcal{P}_2 is minimal, so that reaction values, f_l^* , are found on solving an isostatic problem : they are determined, once C^* is known, by the equilibrium requirement. The

existence of two distinct such solutions implies equality of the criteria in \mathcal{P}_2 , and hence requires one of a finite number of linear combinations, with fixed coefficients (associated with some particular subsets of the lattice), of the random numbers δ_i , to be equal to zero. Such an event has a zero probability. Therefore, *Almost surely, the set C^* of active contacts and the forces f_l^* they carry, are uniquely determined, under a given load, by the initial choice of the random diameters.* As to displacements, lack of uniqueness of the solution to \mathcal{P}_1 is only due to motions such that $\delta u_l = 0$ for any $l \in C^*$.

5 NUMERICAL METHOD

When the number n of grains exceeds a few hundreds, the simplex method proves impracticable, and the solutions to \mathcal{P}_1 and \mathcal{P}_2 , *i.e.*, the displacements and forces have to be determined by different means. In practice, any granular dynamics might be used, provided convergence to the unique equilibrium state is ensured. We found it efficient (7,8) to resort to lubricating viscous forces, of the form

$$f_l = \xi(h_l) \frac{d\delta u_l}{dt},$$

with a decreasing function ξ that possesses a non-integrable divergence as $h \rightarrow 0$. Neglecting inertia, viscous forces balance external forces, and velocities, at each time step, are the solution to a system of linear equations. As $t \rightarrow +\infty$, if the load can be supported, velocities vanish, $f_l \rightarrow f_l^*$ and $h_l \rightarrow 0$ if $l \in C^*$, $f_l \rightarrow 0$ and h_l tends to a finite limit otherwise (this might be proved). Equilibrium is thus asymptotically approached. Even for the largest samples ($n = 12600$) that were studied, the set C^* we obtain always exactly satisfies the isostaticity requirement (8).

6 LARGE SYSTEM LIMIT

Studying many samples of different sizes with various BC's, we check the existence of an RVE, and evaluate its size. The practical procedures are illustrated here in the case

of isotropic compaction, $\sigma = P1$, studied in (8,9).

Intensive quantities describing the internal state of the system should approach a BC-independent limit as $n \rightarrow \infty$. When a systematic dependence on the system diameter L is apparent, one might attribute it to a boundary effect. Near a rigid wall, for instance, fewer contacts are active than in the bulk. Near a free boundary where some stress is imposed, many contacts are active, since all perimeter grains must carry a load. Such boundary influences yield systematic linear variations with $1/L$ (the relative weight of some peripheral zone). Fig. 2 is an illustration of this point, with the proportion of active contacts, N^*/N .

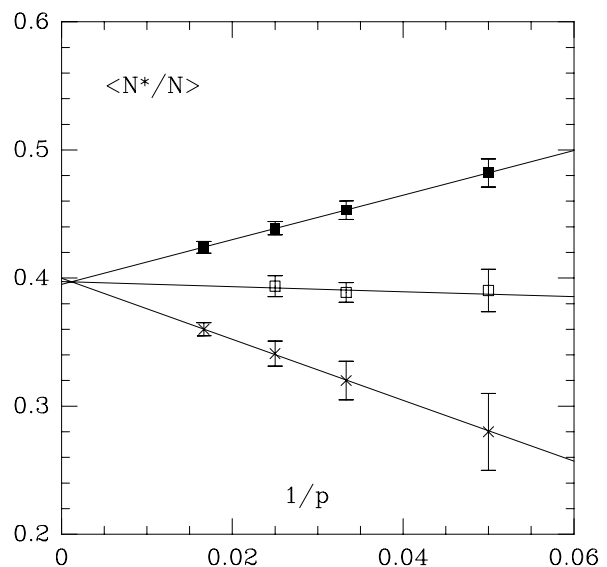


Figure 2: Proportion N^*/N of active bonds, averaged over hexagonal samples with p discs per edge, versus $1/p$, for 3 BC's : rigid rough wall (crosses), periodic BC (open squares), and uniform pressure (black squares). Error bars extend to one sample to sample standard deviation. For periodic BC's, the system has no wall and the limit is reached much sooner. Other BC's are affected by wall effects, hence the linear fits. All data extrapolate to the limit 0.393 ± 0.003 . 32 systems with $p = 60$ ($n > 10000$) were studied.

Fig. 3 is a plot of the probability density of contact forces, $p(f)$. A boundary layer had to be discarded for the data from different BC's to agree. Such wide distributions (see also the 'force chain' pictures in the next section) are commonly observed in granular media (11,13). Some first attempts to predict their shape have been proposed (13,14).

In view of these results, one should obviously avoid thinking in terms of ‘typical contact forces’.

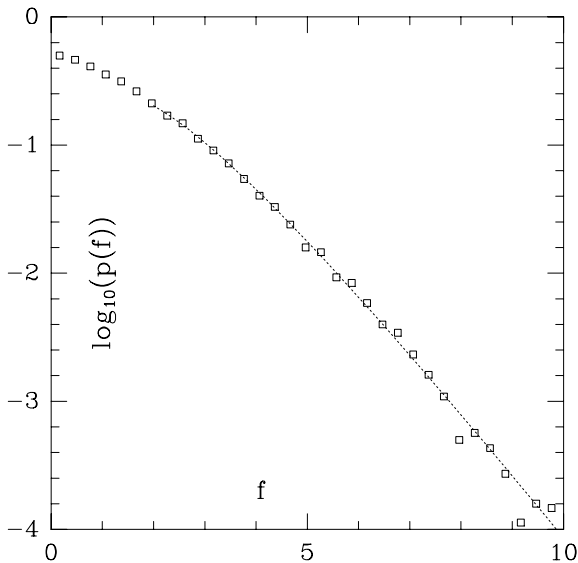


Figure 3: $\log_{10}(p(f))$ versus f in units of aP . $p(f)$ decreases from a finite value for $f \rightarrow 0$. For $f \geq 2$, it might be fitted (dotted line) as $0.92f^{1.5} \exp[-1.28f]$

For the isotropic strain, of the form $\underline{\epsilon} = \lambda \mathbf{1}$, we find $\frac{\lambda}{\alpha} \rightarrow 0.344 \pm 0.003$ as $L \rightarrow \infty$. Equivalently, the maximum packing fraction Φ^* of slightly polydisperse discs, when the diameter distribution is uniform, is, to first order in α

$$\Phi^* = \frac{\pi}{2\sqrt{3}}(1 - k\alpha),$$

with $k = 0.312 \pm 0.006$. Φ^* is well defined here, within the ASD, because of the uniqueness property.

A linear size l might be attributed to the RVE as correlation length for spatial distribution of stress, length scale for local disturbances to attenuate, or depth of a wall effect. All these procedures give $l \sim 10a$.

7 BIAXIAL TEST

If some admissible set of non-negative contact forces exist, then (from section 4) \mathcal{P}_1 and \mathcal{P}_2 both possess a solution, and (as remarked in section 3) another admissible set is then obtained on equating each f_l with the average F_k of all forces carried by the contacts that share the same orientation \mathbf{n}_k . From

eqn. 5, it follows that the system will sustain the load $\underline{\sigma}$ if, and only if, the following conditions hold:

$$\begin{cases} 0 & \leq \sigma_{22} \leq 3\sigma_{11} \\ -\frac{\sigma_{22}}{\sqrt{3}} & \leq \sigma_{12} \leq \frac{\sigma_{22}}{\sqrt{3}}. \end{cases} \quad (11)$$

Keeping $\sigma_{12} = 0$ and $\sigma_{11} + \sigma_{22}$ constant, we have submitted square systems of various sizes (up to 12600 grains, 4 samples) to loads of different directions, with the following values of the ratio $r = \sigma_{11}/\sigma_{22}$: 0.361, 1/2, 2/3, and, 1 being already studied, $\sqrt{3}$, 3, 10. As fig. 4 shows, the anisotropy of the force chains reflects that of the load: as r grows, the contribution of the set C_1 to the transmission of stress increases from negligible to dominant. As the system is anisotropic, only a part of the mechanical behaviour is explored, corresponding, by symmetry, to $\epsilon_{12} = 0$. Due to uniqueness, we obtain strains that functionally depend on load direction, and, thanks to the optimization properties, results can be understood in the following way, illustrated on fig. 5. In the $\epsilon_{11}, \epsilon_{22}$ plane, the sim-

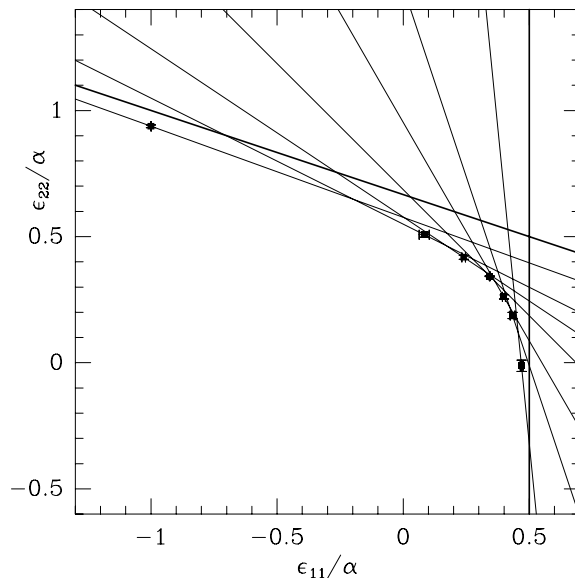


Figure 5: Strain states corresponding to the 7 different load directions that were simulated. Error bars indicate uncertainties in the $L \rightarrow \infty$ extrapolation. The curve $\phi(\epsilon_{11}, \epsilon_{22}) = 0$ is the envelope under the tangents that are drawn for each point. The asymptotes are the thick straight lines.

plex of possible displacements (from eqns. 7, strains are linear combinations thereof) projects onto a simplex. As the system size L

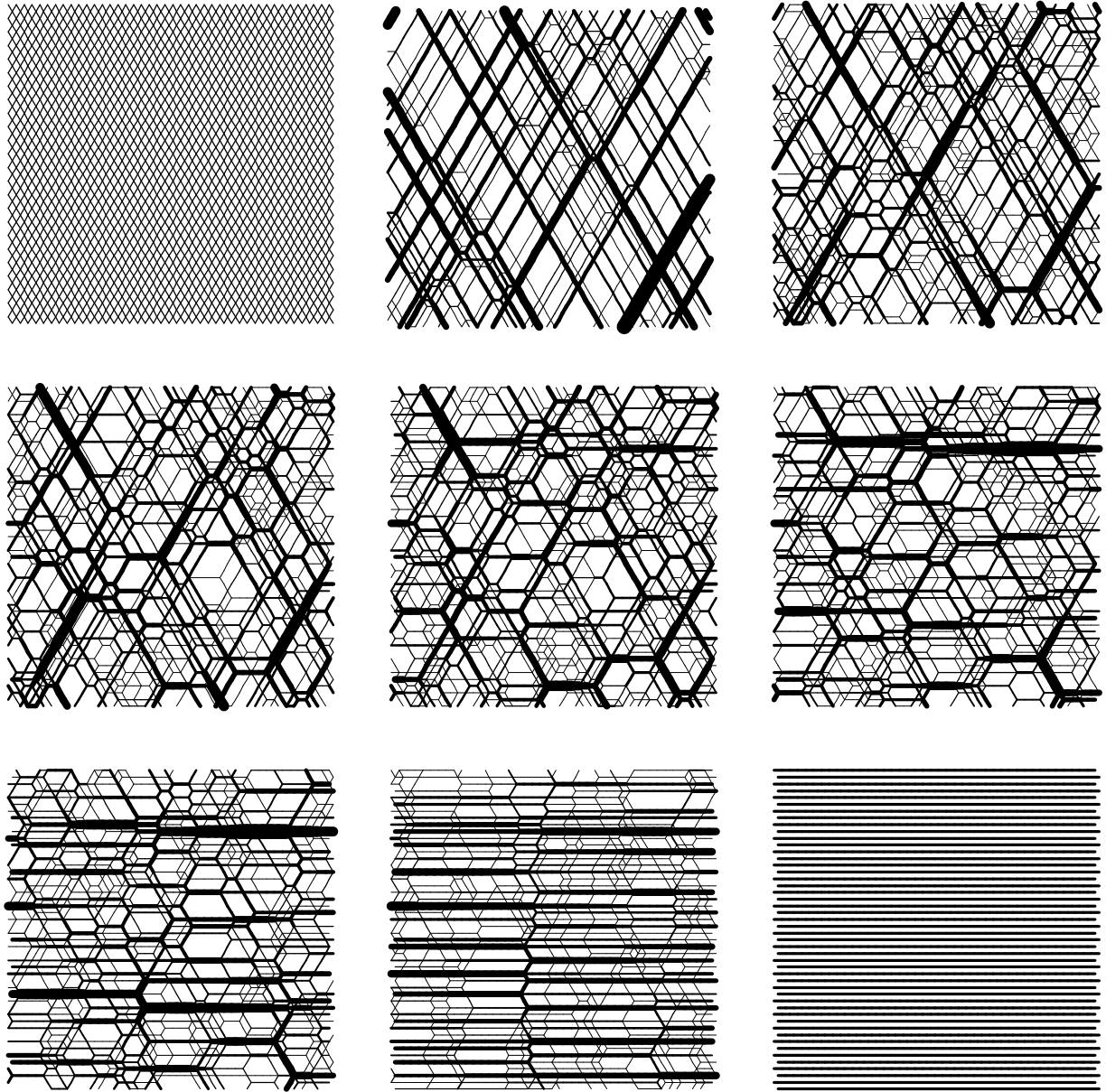


Figure 4: Aspect of the sets of force-carrying contacts. From left to right and from top to bottom r grows from $1/3$ to ∞ , taking the values given in the text. Active contacts are drawn as lines joining disc centres, with a thickness proportional to the force intensity.

increases, the number of linear sections limiting this plane simplex tends to infinity, while their lengths tend to zero. Consequently, in the limit $L \rightarrow \infty$ of macroscopic systems, the set of strains $\epsilon_{11}, \epsilon_{22}$ that are permitted by grain impenetrability is limited by some smooth curve $\phi(\epsilon_{11}, \epsilon_{22}) = 0$. For any sustainable load (with $\sigma_{12} = 0$), $\sigma_{11}\epsilon_{11} + \sigma_{22}\epsilon_{22}$, the criterion of problem \mathcal{P}_1 , is maximized on that curve, where its tangent is orthogonal to the vector of coordinates $(\sigma_{11}, \sigma_{22})$. The existence of this point is equivalent to load sustainability, and the curve has therefore two asymptotes that are orthogonal to the

marginally supported loads given by eqn. 11 ($r = 1/3$ and $r = +\infty$). The BC's require all contacts of C_1 to close for $r \rightarrow +\infty$, hence $\epsilon_{11} = \lambda_1 = \alpha/2$, and all contacts of C_2 and C_3 to close for $r = 1/3$, hence $\lambda_2 = \lambda_3 = \alpha/2$, and $\epsilon_{22} = (2/3)\alpha - (1/3)\epsilon_{11}$. Note that, as sample surface area is only minimized for an isotropic pressure, the system naturally exhibits dilatancy. Our numerical results strongly suggest that an RVE always exists, except right on the limit of the domain of supported loads, for $\sigma_{22} = 0$ or for $\sigma_{11} = \sigma_{22}/3$ (the statistical properties of the sets of active contacts depending then, and

only then, on the specific type of BC). For a given value of α , the ASD should eventually break down as the curve approaches any one of its asymptotes (the later the smaller α).

Fig. 6 is a plot, versus $1/r$, of the proportion of active contacts in the different directions. The typical aspect of force prob-

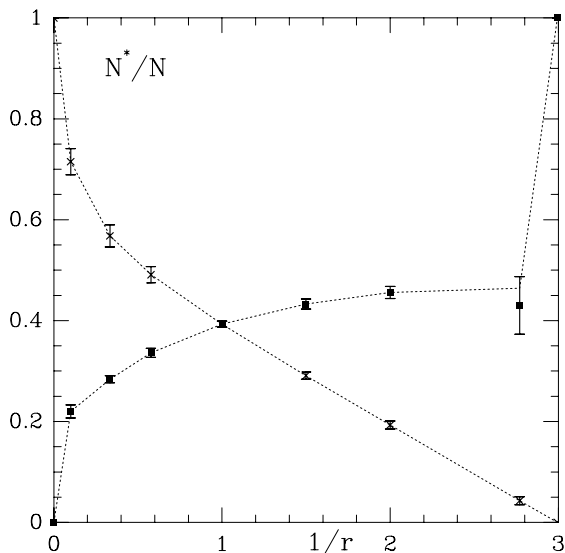


Figure 6: Proportion of contacts in direction 1 (crosses) and 2 and 3 (squares) that are active, versus $1/r$. The dotted lines are guides to the eye.

ability densities p_k , depending on the direction $k = 1, 2, 3$ of the contact, in the case of an anisotropic load, is displayed on fig. 7, in the case $r = 1/2$. In this case, $F_3 = F_2$, $p_3 = p_2$ and $F_1 = F_2/4$. The anisotropy influence on the force distribution decreases with the force intensity. Most force chains carrying large efforts are oriented along the principal axis of stress with the higher eigenvalue ($p_1(f) \ll p_2(f)$ at large f) while the smallest contact forces remain isotropically distributed ($p_1(f) \simeq p_2(f)$ for small f). A similar tendency was noted by other authors (12).

8 DISCUSSION

Thanks to the simplicity of the model and the efficiency of the numerical method, we derive, from grain-level simulations, a macroscopic constitutive law for biaxial compression. The existence of an RVE (of typical size $l \sim 10a$) is unambiguously established,

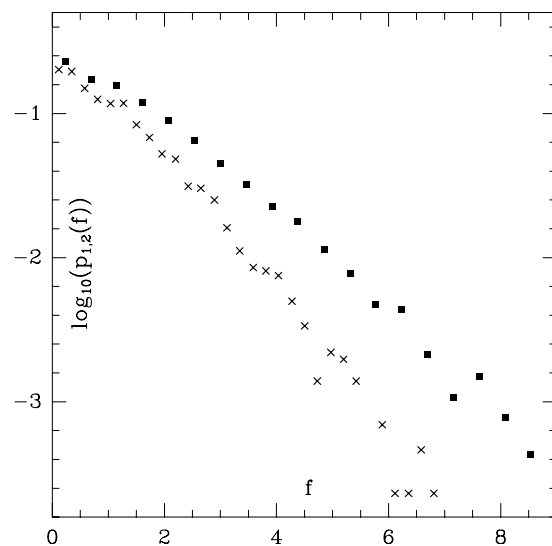


Figure 7: $\log_{10}(p_1(f))$ (crosses) and $\log_{10}(p_2(f))$ (squares) when $r = 1/2$, versus f , the unit of force being $a(\sigma_{11} + \sigma_{22})/2$.

and the force distribution is accurately computed. Load anisotropy mainly affects the orientation of the largest contact forces.

Force chains, wide force distributions, redistribution of contacts on altering the load direction, are now recognized as characteristic features of granular materials. The simple model we study should provide a convenient test for theories attempting a quantitative prediction of such phenomena.

Because of the 3 basic assumptions, the model also exhibits some special properties, the general relevance of which deserves to be discussed. One is the *uniqueness* of the equilibrium state. However conceptually appealing (we are dealing with a well-posed problem, the use of one or another algorithm does not bias the choice of a particular type of solution, etc...), it is certainly unrealistic, for it leads to a one to one correspondance between (sustainable) stress direction and strain. This excludes plasticity and dissipation. Submitted to a quasi-static cyclic load, the model material goes, back and forth, through the same states, without any irreversible evolution and any energy dissipation. Moreover, the marginally supportable stresses are associated with very peculiar, ordered, spatial distribution of forces. Although the system exhibits such "realistic" behaviours as *dila-*

tancy and contact reorientation, its relevance as a model for usual biaxial experiments is likely to be limited to the *reversible* part of the stress-strain curve. It shows that, *if the geometry of the packing is such that the set of active contacts might change significantly with small grain displacements, the "elastic" part of the elastic-plastic behaviour is not necessarily due to the elasticity of the grains.*

Another remarkable property is the *isostaticity* in the equilibrium state. In (9) it is shown that, if one dispenses with the ASD, though the uniqueness is lost, one still finds an isostatic force-carrying structure at equilibrium. As special lattice alignments disappear on taking real, finite displacements into account, it is isostaticity in a generic sense, with a coordination number, counting only load-carrying discs (n^*) and active contacts (N^*), of 4. This seems to hold quite generally, and adding some Coulomb friction, the inequality $N^* < 2n^*$ should persist. Therefore, *the coordinance of a generic packing of rigid discs in 2 dimensions (or rigid spheres in 3 dimensions) should never exceed 4 (respectively: 6).*

The isotropic compaction of the same system made of *elastic* discs is studied in (10). The increase, as pressure grows, of the density of active contacts, results in a gradual loss of the characteristic stress heterogeneity of granular materials.

In future work, with more sophisticated models, we intend to introduce (separately, at first) three features that are possible microscopic sources of plasticity and dissipation: solid friction, large displacements of the grains, non-convex attractive potential between the grains (cohesion). Any one of those ingredients destroys the uniqueness property, and is thus likely to yield an incremental macroscopic behaviour (as opposed to a functional relationship between stress and strain). In particular, it is expected that, provided significant granular rearrangements occur on small scale, the "plastic" part of the elastic-plastic behaviour is not necessarily due to intergranular friction.

REFERENCES

1. Thornton C., ed. (1993). *Powders & Grains 93*, Balkema, Rotterdam.
2. Wolf D.E. & Grassberger P. eds. (1997). *Friction, Arching, Contact Dynamics*. World Scientific, Singapore (to appear)
3. Dantu P (1957) *Proc. 4th Int. Conf. on Soil Mech. and Foundation Engineering*, 144.
4. Josselin de Jong G. & A. Verruijt A. (1969). *Cahiers du Groupe Français de Rhéologie*, **2**, 73.
5. Nemat-Nasser S. & Hori M. (1993). *Micromechanics : overall properties of heterogeneous materials*, North-Holland
6. Behringer R.P. & Jenkins J.T. (1997). *Powders & Grains 97*, Balkema, Rotterdam (to appear)
7. Ouaguenouni S. & Roux J.-N. (1995). *Europhys. Lett.* **32**, 449
8. Ouaguenouni S. & Roux J.-N. (1996), submitted to *Europhys. Lett.*
9. Ouaguenouni S. & Roux J.-N. (1997), in ref. 2.
10. Roux J.-N. (1997), in ref. 6.
11. Radjai F., Jean M., Moreau J.-J. & Roux S. (1996). *Phys. Rev. Lett.* **77**, 274-277
12. Radjai F. , Wolf D., Roux S., Jean M. & Moreau J.-J. (1997), in ref. 2.
13. Liu C. H., Nagel S. R., Schecter D. A., Coppersmith S. N., Mujumdar S., Narayan O. & Witten T.A. (1995). *Science* **269**, 513
14. Coppersmith S.N., Mujumdar S., Narayan O. & Witten T.A. (1996). *Phys. Rev. E*, **53**, 4673
15. Cambou B. (1993), in ref. 1.